Giant enhancement of dynamic conductance in molecular devices

Junling Wu,[1] Baigeng Wang,[2] Jian Wang,[1,*] and Hong Guo[3]
[1]*Department of Physics, The University of Hong Kong, Pokfulam Road, Hong Kong, China*
[2]*National Laboratory of Solid State Microstructures and Department of Physics, Nanjing University, Nanjing 210093, China*
[3]*Department of Physics, McGill University, Montreal, Quebec, Canada H3A 2T8*
(Received 5 July 2005; revised manuscript received 8 September 2005; published 14 November 2005)

We report theoretical investigations of dynamic conductance of molecular systems in the metal-molecule-metal device configuration. The quantum coherent ac transport may be mediated by resonant states extending the entire molecule, or mediated by localized states within the molecule itself. The latter is characterized by tiny features in the dc conductance, but the dissipative part of dynamic conductance can be enhanced by several orders of magnitude as the ac frequency is increased. This phenomenon can be understood from an analytical model.

DOI: 10.1103/PhysRevB.72.195324 PACS number(s): 73.63.−b, 71.20.Tx, 85.35.−p

Anticipating a variety of technological applications, molecular scale conductors and devices are the subject of increasingly more research in recent years.[1] Experimentally, device configurations of metal-molecule-metal can be established by forming a molecular moiety between two metal electrodes,[2,3] or by contacting a self-assembled monolayer of molecules (SAM) with a conducting atomic force microscope (AFM) tip.[4] Extensive transport data under a dc bias voltage has been collected which provides important understanding of the operation of molecular electronics or moltronics. One of the most important issues of moltronics concerns the control of device conductance by an external parameter, for instance, if a sensitive control could be achieved by an external gate voltage, a molecular scale field effect device would be possible. Unfortunately, for short molecules this proves to be very difficult, as recent experimental data[5,6] showed that dc conductance for short molecules can be varied for about a factor of 10 or less via gate voltage because electric field lines are effectively screened by the metal leads nearby. This is far from viable to be a useful technology, although for long molecules such as carbon nanotubes, good gate control of conductance appears possible.[7]

In this paper, we present a theoretical analysis which shows that a critical control of conductance of short molecules can be achieved by a finite frequency ac bias. In fact, relatively little is known about transport properties of molecular devices under a high frequency ac bias[8] which is itself a very important and difficult problem[9] of quantum transport theory, and a first principles self-consistent analysis of finite frequency dynamic conductance for the metal-molecule-metal device configuration, including all atomic details of the molecule as well as the leads, has not yet been carried out. Indeed, for several molecular tunnel junctions, our calculations suggest (see below) a very surprising and potentially important result that there exists a giant enhancement of dynamic conductance, by many orders of magnitudes, as a function of the ac frequency. This prediction and its associated physical mechanism, as well as other results, will be presented. The phenomenon of this giant dynamic conductance enhancement can also be understood analytically.

To begin, we briefly outline the theoretical approach. We consider the typical metal-molecule-metal device configuration shown schematically in the top panel of Fig. 1 and apply the *ab initio* technique of Ref. 10 where density functional theory (DFT) is carried out within the Keldysh nonequilibrium Green's function (NEGF) formalism. We use a *s*, *p*, *d* real space LCAO basis set[10,11] and define the atomic core by standard nonlocal norm conserving pseudopotential.[12] The density matrix of the device is constructed via NEGF and the semi-infinite leads provide real space potential boundary conditions for the Kohn-Sham (KS) potential of the device scattering region, this region consists of the molecule plus several layers of the metal leads. The KS potential includes contributions from Hartree, exchange, correlation, the atomic core, and any other external potentials. The NEGF-DFT iteration is numerically converged to 10^{-4} eV which we deter-

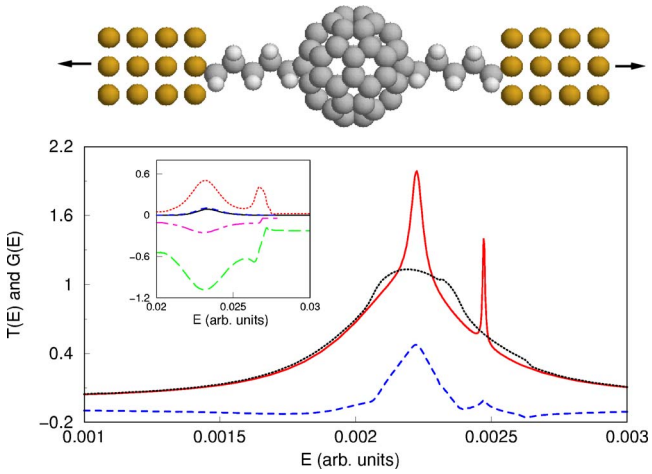

FIG. 1. (Color online) Top, schematic plot of a metal-molecule-metal tunnel junction. Main plot and its inset, dynamic conductance G and dc transmission coefficient $T(E)$ (solid line) vs electron energy E at different frequencies. In the main plot the dotted line is for G_R and the dashed line corresponds to G_I at ν=0.001 a.u. The inset is the plot in a larger energy range. Here the symbols correspond to solid line [$T(E)$], dashed line (G_R at ν=0.001 a.u.), dotted line (G_R at ν=0.005 a.u.), long-dashed-short-dashed line (G_I at ν=0.001 a.u.), long-dashed line (G_I at ν=0.005 a.u.).

mine to be reasonable for our purpose. For analyzing dynamic conductance, the NEGF-DFT formalism produces all the NEGF as well as equilibrium Green's functions needed (see below).

Next, we evaluate dynamic conductance of the device using the NEGF based transport formalism of Ref. 13, where the general expression for dynamic conductance was derived to be (setting electron charge q and reduced Planck constant $\hbar$ to unity),

$$G_{\alpha\beta}(\omega) = G^c_{\alpha\beta} - G^d_\beta \sum_\gamma G^c_{\alpha\gamma} \Big/ \left(\sum_\gamma G^d_\gamma \right), \tag{1}$$

where the subscripts α, β denotes the leads, ω is the ac frequency. The first term $G^c_{\alpha\beta}$ is the dynamic conductance due to particle current alone,

$$G^c_{\alpha\beta}(\omega, E) = -\int \frac{dE_1}{2\pi} \frac{f-\bar{f}}{\omega} \mathrm{Tr}(-\bar{\mathcal{G}}^r \Gamma_\beta \mathcal{G}^a \Gamma_\alpha + \bar{\mathcal{G}}^r \Gamma \mathcal{G}^a \Gamma_\alpha \delta_{\alpha\beta} - i\omega \bar{\mathcal{G}}^r \mathcal{G}^a \Gamma_\alpha \delta_{\alpha\beta}), \tag{2}$$

here $\mathcal{G}^r$ is the retarded equilibrium Green's function of the device which we evaluate using the NEGF-DFT technique discussed above;[10] $\bar{\mathcal{G}}^r = \mathcal{G}^r(E_+)$ with $E_+ = E_1 + \omega$; and $\bar{f} \equiv f(E_+)$ where f is the Fermi distribution function. The quantity Γ_α is the linewidth function which gives coupling of the device to lead α, and is calculated by evaluating the self-energy of the semi-infinite atomic leads.[10] Here $\Gamma = \Sigma_\alpha \Gamma_\alpha$. The second term in Eq. (1) is the contribution from the displacement current due to electrodynamics where the quantity

$$G^d_\beta = i \int \frac{dE_1}{2\pi} (f - \bar{f}) \mathrm{Tr}(\bar{\mathcal{G}}^r \Gamma_\alpha \mathcal{G}^a). \tag{3}$$

Therefore, for any molecular devices, once the Green's functions of the device scattering are obtained from the NEGF-DFT analysis,[10] Eqs. (1)–(3) allows one to evaluate the frequency dependent conductance. Several molecular tunnel junctions in the form of Fig. 1 will now be analyzed. Unless otherwise specified, we use atomic units where angular frequency $\omega = 1$ corresponds to frequency $\nu = 6.57 \times 10^{15}$ Hz and 1 a.u. of energy is 27.2 eV.

First, we consider the ac response of an Al-C_{60}-Al tunnel junction.[15,16] For a model analysis, we fixed the C_{60} molecule at a distance $d = 4.23$ Å from the lead surface. The value of d as well as the entire device structure, should in principle be determined under the ac transport condition self-consistently. This is however an unsolved problem as one does not yet know how to calculate quantum mechanical forces under an ac current flow. We therefore neglect this piece of physics as an approximation for our model analysis. We use a value of d that is larger than the equilibrium bond length so that a clear tunneling regime is established for which we can provide a good analytical derivation later in the paper. A large junction distance may be realized by connecting the C_{60} molecule to the leads through a highly resistive CH_2 molecular chain (see Fig. 1), which we have also calculated and found similar results for the dynamic conductance.

The lower panel of Fig. 1 plots the real and imaginary part of the ac conductance, $G_R \equiv \mathrm{Re}(G_{11})$ and $G_I \equiv \mathrm{Im}(G_{11})$ vs

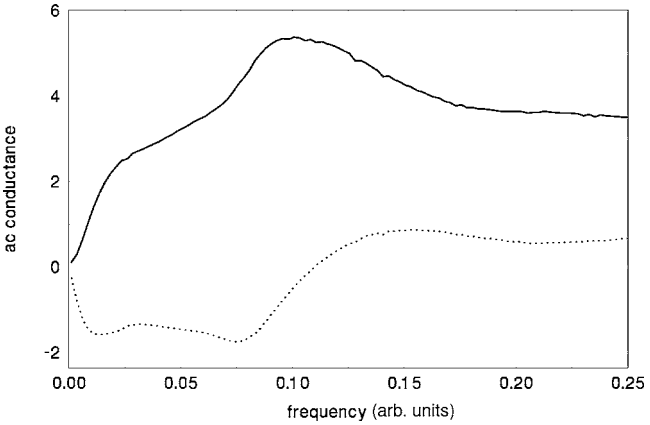

FIG. 2. G vs ν for the C_{60} device at $E = 0.0234$ a.u.

electron energy at two finite ac frequencies $\omega = 0.001$ a.u. and 0.005 a.u.[17] When $\omega = 0$, G_{11} simply reduces to the usual dc conductance given by transmission coefficient $T = T(E)$ (shown as solid line). A resonant transport behavior through the device can be identified by the sharp peaks in $T(E)$. In fact, for this molecular system there are two types of peaks, those with $T \geqslant 1$ and those for $T \ll 1$. Then, at finite ω, ac response is rather different for these two kinds of resonances. At $E = 0.002\,34$ a.u., there are two perfect transmission channels resulting $T = 2$. Similarly, at $E = 0.002\,48$ a.u. there are three partially transmitting channels giving $T \approx 1.5$. For these resonancelike peaks of $T \geqslant 1$, a finite ω strongly suppresses the ac conductance, and a larger ω gives a larger suppression. The imaginary part G_I shows a typical inductivelike behavior near a strong resonance energy but becomes capacitivelike away from it.[14]

The most important finding is the behavior of ac conductance at the $T \ll 1$ peak features, for example, at $E = 0.023\,32$ a.u. where $T \sim 0.09$ (see inset of Fig. 1), the ac conductance G_R increases by a large factor upon increasing ω, i.e., G_R increases from 0.09 at $\omega = 0$ to 0.5 at $\omega = 0.005$ a.u. Even much larger enhancement of G_R can be obtained, for instance at $E = 0.0268$ a.u. there is a tiny feature in $T(E)$ ($T \sim 2 \times 10^{-4}$, too small to be resolved in the solid line of the inset of Fig. 1), but at $\omega = 0.0005$ a.u. this feature is "amplified" to a clear peak of $G_R \approx 0.04$, a giant enhancement by a factor of ~ 200. This behavior is more clearly shown in Fig. 2 which plots ac conductance vs ω fixing $E = 0.0234$ a.u. It is clear that G_R (solid line) increases sharply from essentially zero to a large value at finite ω. The enhancement is quite general. For instance, Fig. 3 plots the ac conductance vs Fermi energy for a C_{60} tunnel junction with CH_2 end groups[18] (see top panel of Fig. 1), a giant G_R enhancement of four orders of magnitude were found. In Fig. 4, we depict G_R vs frequency. We see that G_R rises sharply as the frequency is turned on.

The giant enhancement of ac conductance by a finite frequency is a very important feature for molecular electronics theory and its potential application. Our *ab initio* data showed that ac frequency may well provide a critical external control of quantum transport for single molecule conduction. Although the frequency is in the microwave range, experimental verification of this prediction may be possible.

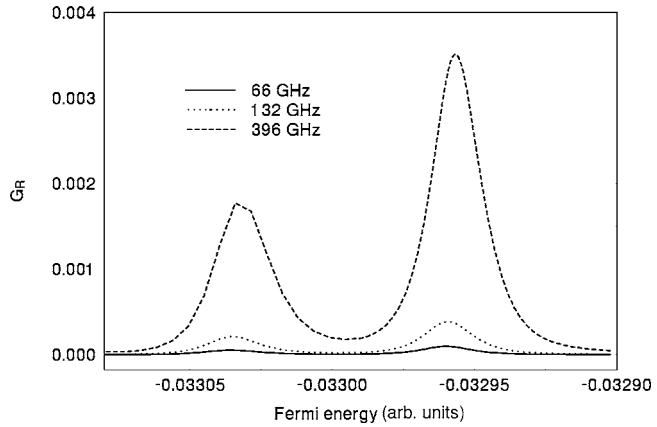

FIG. 3. G_R vs Fermi energy for the $5CH_2$-C_{60}-$5CH_2$ device at different frequencies.

Indeed, oscillation up to 712 GHz has been achieved in InAs/AlSb resonant tunneling diodes by Brown *et al.*[19] Recently, a single-walled carbon nanotube transistor operated at 2.6 GHz has been demonstrated.[20] In the following, we provide an analytical understanding of the above phenomenon. We first recognize that the giant dynamic conductance enhancement for features where $T \ll 1$ cannot come from resonance transmission through a single level. Even though resonance transmission can give $T \ll 1$, for instance when the molecule couples to the leads in an extremely asymmetrical way, our calculation showed that G_R is drastically reduced for this situation, not enhanced, by a finite ac frequency. The small values of $T(E)$ can come from another possibility, namely from tunneling through spatially localized states of the scattering region of the device.

All the qualitative features of the giant dynamic conductance enhancement can indeed be obtained as mediated by localized states. We now demonstrate this using a coupled "quantum dot" (QD) device in contact with two leads. Each QD has its own localized state with level ϵ_i $(i=1,2)$ when the QDs weakly interact with a tunnel coupling parameter t. The Hamiltonian of this system is given by a 2×2 matrix H_{ij}, with $H_{11}=\epsilon_1$, $H_{22}=\epsilon_2$, and $H_{12}=H_{21}=t$. The coupling to the leads is given by the linewidth matrix Γ_{ij} with $\Gamma_{11}=\Gamma_L$, $\Gamma_{22}=\Gamma_R$, and $\Gamma_{12}=\Gamma_{21}=0$. The retarded Green's function $\mathcal{G}^r$ of this system is $\mathcal{G}^r=(E-H+\Sigma)^{-1}$. Here Σ is the self-energy due to coupling to the leads, $\Sigma_\alpha=-i\Gamma_\alpha/2$. The dc transmission coefficient T is then obtained by taking the $\omega\to 0$ limit of Eq. (2). For symmetric coupling $\Gamma_L=\Gamma_R=\Gamma/2$ and symmetric QDs $\epsilon_1=\epsilon_2=\epsilon$, the result is

$$T(E)=\frac{|t|^2\Gamma^2/4}{[(E-\epsilon)^2+\Gamma^2/16-t^2]^2+t^2\Gamma^2/4}. \tag{4}$$

This dc transmission line shape, due to the two localized states, has two distinct behaviors. First, for parameters $t>\Gamma/4$, two resonance transmission peaks with large coefficients $T=1$ are found at $E=\epsilon\pm\sqrt{t^2-\Gamma^2/16}$. The fact of resonance transmission can be easily established by checking the poles of Eq. (4). Second, when $t<\Gamma/4$, T has a single peak at $E=\epsilon$ with a value

$$T=\frac{t^2\Gamma^2/4}{(\Gamma^2/16-t^2)^2+t^2\Gamma^2/4}<1. \tag{5}$$

This transmission peak value can actually be much less than unity for very small t. The reason for small T as well as for only one peak in T can both be understood as follows. For small tunnel coupling $t<\Gamma/4$, the individual QD states ϵ_i has little overlap, thus they are spatially localized inside the two QDs. This gives rise to small T because the two localized states do not couple well, and it gives only one peak in T because for the symmetric system $\epsilon_1=\epsilon_2=\epsilon$. We therefore conclude that the transport behavior of $T=1$ is due to resonance transmission, and that of $T<1$ is due to transport through localized states. These behaviors in dc transmission are similar to those of the molecular tunnel junction data discussed above.

Now we examine the ac response of the coupled QD system using Eq. (1). An analytical solution is possible for small t limit $(t\ll\Gamma)$ so that $T\ll 1$. On the other hand, for large t the dynamic conductance can only be calculated by numerically evaluating Eq. (1). Setting $G=G_{11}=-G_{12}$ and $\Gamma_L=\Gamma_R$, we found that when $E=\epsilon$ the dynamic conductance is

$$G=\frac{-\Gamma_L}{4\pi(\Gamma_L-i\omega)}(X_1+iX_2)+O(t^2) \tag{6}$$

with

$$X_1=\log\frac{\Gamma_L^2}{4\omega^2+\Gamma_L^2} \quad \text{and } X_2=2\tan^{-1}\frac{2\omega}{\Gamma_L}. \tag{7}$$

These results show clearly that $G_R=0$ when $\omega=0$, and G_R increases to much larger values at finite ω. This is exactly what was observed for the molecular tunnel junctions. More precisely, by numerically evaluating Eq. (1), we plot in Fig. 5 G_R and G_I (measured in e^2/h) vs ω for the double QD by setting $t\sim 0$ and $E=\epsilon$. Figure 5 shows clearly that as the frequency is turned on, the device starts to conduct where G_R increases very shapely and reaches a maximum value $2e^2/h$ at $\omega_{\max}\sim 1.1\Gamma_L$ and then decreases slowly. Except the scale of frequency ω which depends on system energetics, the qualitative features of Fig. 2 for molecular devices and Fig. 5 are the same. ac transport mediated by localized states in the

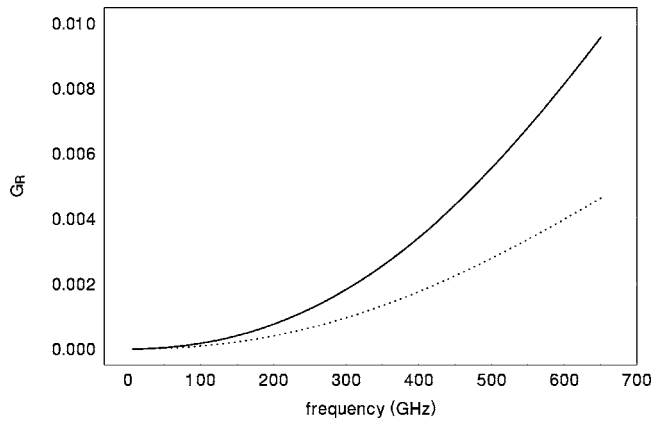

FIG. 4. G_R vs frequency ν for the $5CH_2$-C_{60}-$5CH_2$ device at different Fermi energies $E=-0.032\,96$ a.u. and $-0.033\,035$ a.u.

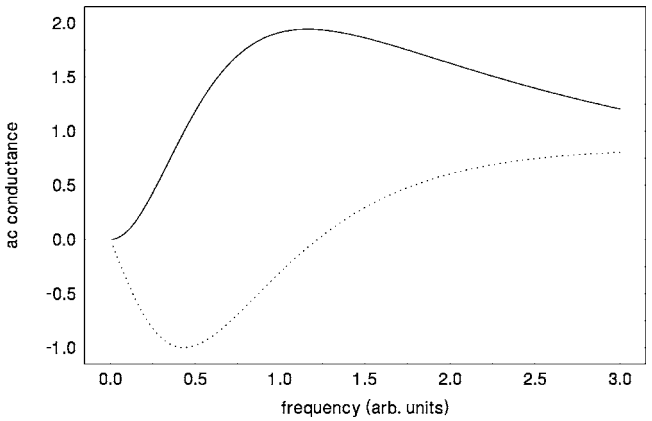

FIG. 5. G vs ω for the coupled QD model. Solid line, G_R; dotted line, G_I.

molecular junction may therefore give rise to very large conductance enhancement by a finite frequency ac bias.

A qualitative discussion of dynamical conductance from a classical circuit model[21] is also worthwhile. For the resonant peak with $T \geqslant 1$ which is very conductive, the molecular junction can be considered as an inductor in series with a resistor, i.e., a R-L circuit; on the other hand, for $T \ll 1$ which is nonconductive, the device responses like a capacitor, i.e., a R-C circuit. Classically, the dynamic conductance can be written in the following form up to second order of frequency ω:

$$G_{RL}(\omega) = \frac{1}{R} + i\frac{\omega L}{R^2} - \frac{\omega^2 L^2}{R^3} \tag{8}$$

and $G_{RC}(\omega) = -i\omega C + \omega^2 C^2 R$. Hence for a R-L circuit, the real part of the dynamic conductance G_R decreases when the frequency is switched on; and for a R-C circuit, the dc conductance is zero but as the frequency is turned on, G_R increases.

Finally, we note that in this paper we have focused on an individual device under an external ac field. The resistance and capacitance of this individual device determine its ac response. In an actual application, this device will be put into a circuit where there are other devices, metal gates and interconnect wires which give rise to some stray capacitances from this device. In this paper, we neglected these stray capacitances which depend on details of the circuit layout. Depending on the impedance R of the device and the stray capacitance, there might be a problem of cutoff frequency in our device. This is because if the impedance of the device is much larger than that of the stray capacitance, the current will not go through the device. This could happen at high frequency. We note that this cutoff frequency $\Omega \sim 1/RC$ for our nanodevice may be very high. This is because there is an intrinsic capacitance in our device. This intrinsic capacitance is very small, on the order of aF ($10^{-18}F$) or even smaller.[22] For a classical nanocapacitor with a plate area of $S = 10\ \mathrm{nm}^2$ and distance $d = 1$ nm, we can estimate $C = \epsilon_0 S/d$ gives $10^{-19}F$. The precise value of this intrinsic capacitance is difficult to calculate and varies with device details,[23] but the classical estimate gives a rough idea. From our calculation, the intrinsic capacitance has the following effect: at low frequency, the impedance is dominated by the large resistance (around 10 Mohm); as the frequency is increased the impedance quickly decreases (the dynamic conductance quickly increases). Therefore, effectively at high frequency the "impedance" $R(\omega)$ of our device is much smaller. This will bring up the cutoff frequency drastically. Since our device and the whole circuit are on the nanoscale, the stray capacitance should not be too far from the intrinsic capacitance. We now estimate the cutoff frequency from $\Omega \sim 1/RC_{\mathrm{stray}}$ which depends very much on R and C_{stray}. At high frequency, it is reasonable to use $R(\omega) \sim 0.1$ MOhm. If we use $C_{\mathrm{stray}} \sim 10^{-17}F$ which is two orders of magnitude larger than the intrinsic capacitance of our device, we obtain $\Omega = 1000$ GHz.

In summary, we found that for molecular scale conductors in the form of metal-molecule-metal, the quantum coherent ac transport may be mediated by resonant states extending the entire molecule as well as by localized states within the molecule itself. The latter is characterized by tiny features in the dc conductance. The dissipative part of dynamic conductance G_R is found to have a giant enhancement, by several order of magnitude, as ac frequency is increased. The physical picture is supported by an analytical model. These results allow us to expect that ac transport properties of molecular devices have much to offer for practical applications.

We gratefully acknowledge financial support from RGC Grant No. HKU 7032/03P of the HKSAR (J.W.), from NSFC under Grant No. 90303011 (B.G.W.), and from NSERC of Canada, FCAR of Quebec, and NanoQuebec (H.G.).

*Electronic address: jianwang@hkusub.hku.hk

[1] C. Joachim, J. K. Gimzewski, R. R. Schlittler, and C. Chavy, Phys. Rev. Lett. **74**, 2102 (1995); A. Yazdani, D. M. Eigler, and N. Lang, Science **272**, 1921 (1996); M. A. Reed, C. Zhou, C. J. Muller, T. P. Burgin, and J. M. Tour, Science **278**, 252 (1997); S. J. Tans, A. R. M. Verschueren, and C. Dekker, Nature (London) **393**, 49 (1998). For recent reviews, see for example, M. A. Ratner, Mater. Today **2002**, 20 (Feb. 2002 issue); C. Joachim, J. K. Gimzewski, and A. Aviram, Nature (London) **408**, 541 (2000); J. R. Heath and M. A. Ratner, Phys. Today **56** (5), 43 (2003); A. Nitzan and M. A. Ratner, Science **300**, 1384 (2003).

[2] W. Wang, T. Lee, and M. A. Reed, Phys. Rev. B **68**, 035416 (2003).

[3] R. H. M. Smit, Y. Noat, C. Untiedt, N. D. Lang, M. C. van Hemert, and J. M. van Ruitenbeek, Nature (London) **419**, 906 (2002).

[4] D. J. Wold and C. D. Frisbie, J. Am. Chem. Soc. **122**, 2970 (2000); D. J. Wold and C. D. Frisbie, J. Am. Chem. Soc. **123**, 5549 (2001); J. M. Beebe, V. B. Engelkes, L. L. Miller, and

C. D. Frisbie, *ibid.* **124**, 11268 (2002); X. D. Cui, X. Zarate, J. Tomfohr, O. F. Sankey, A. Primak, A. L. Moore, T. A. Moore, D. Gust, G. Harris, and S. M. Lindsay, Nanotechnology **13**, 5 (2002); J. Zhao and K. Uosaki, Nano Lett. **2**, 137 (2002).

[5] J. Lee, G. Lientschnig, F. Wiertz, M. Struijk, R. A. J. Janssen, R. Egberink, D. N. Reinhoudt, P. Hadley, and C. Dekker, Nano Lett. **3**, 113 (2003).

[6] C. R. Kagan, A. Afzali, R. Martel, L. M. Gignac, P. M. Solomon, A. G. Schrott, and B. Ek, Nano Lett. **3**, 119 (2003).

[7] S. J. Wind, J. Appenzeller, R. Martel, V. Derycke, and Ph. Avouris, Appl. Phys. Lett. **80**, 3817 (2002).

[8] C. Roland, M. Buongiorno Nardelli, J. Wang, and H. Guo, Phys. Rev. Lett. **84**, 2921 (2000); C. C. Wan, Jóse-Luis Mozos, Jian Wang, and Hong Guo, Phys. Rev. B **55**, R13393 (1997); W. Zheng, Y. Wei, J. Wang, and H. Guo, Phys. Rev. B **61**, 13121 (2000).

[9] M. Büttiker, A. Prêtre, and H. Thomas, Phys. Rev. Lett. **70**, 4114 (1993).

[10] The NEGF-DFT package MCDCAL is discussed in J. Taylor, H. Guo, and J. Wang, Phys. Rev. B **63**, 245407 (2001); J. Taylor, H. Guo, and J. Wang, Phys. Rev. B **63**, 121104(R) (2001).

[11] M. Brandbyge, J. -L. Mozos, P. Ordejón, J. Taylor, and K. Stokbro, Phys. Rev. B **65**, 165401 (2002).

[12] D. R. Hamann, M. Schlüter, and C. Chiang, Phys. Rev. Lett. **43**, 1494 (1982).

[13] B. Wang, J. Wang, and H. Guo, Phys. Rev. Lett. **82**, 398 (1999). The NEGF based ac transport theory of this paper has been shown to be equivalent to the scattering matrix theory (Ref. 9), but is more convenient for the numerical procedure.

[14] M. Buttiker and T. Christen, in *Mesoscopic Electron Transport*, edited by L. L. Sohn, L. P. Kouwenhoven, and G. Schon (Kluwer Academic, Dordrecht, 1997), p. 259.

[15] In our calculations, an Al electrode is composed of unit cells with nine Al atoms oriented in the (100) direction repeated to $\pm\infty$. The scattering region contains four layers of the Al atoms on either side of the molecule.

[16] The dc transport has been studied in Ref. 10.

[17] The Fermi energy can be shifted using the gate voltage. This has been demonstrated experimentally for carbon nanotubes [see S.B. Cronin, R. Barnett, M. Tinkham, S.G. Chou, O.Rabin, M.S. Dresselhaus, A.K. Swan, M.S. Unlu, and B.B. Goldberg, Appl. Phys. Lett. 84, 2052 (2004)].

[18] The distance between CH_2 and Al is chosen to be $d=1.9$ Å. Since CH_2 has a large resistance, our result is not very sensitive to d.

[19] E. R. Brown and J. R. Soderstrom, Appl. Phys. Lett. **58**, 2291 (1991).

[20] S. D. Li, Z. Yu, S. F. Yen, W. C. Tang, and P. J. Burke, Nano Lett. **4**, 753 (2004).

[21] A. Pretre, H. Thomas, and M. Buttiker, Phys. Rev. B **54**, 8130 (1996).

[22] J. G. Hou, B. Wang, J. Yang, X. R. Wang, H. Q. Wang, Q. Zhu, and X. Xiao, Phys. Rev. Lett. **86**, 5321 (2001). In this paper, the capacitance between an atomic cluster and substrate in a tunnel junction is experimentally found to be $0.26aF$.

[23] J. Wang, H. Guo, J. L. Mozos, C. C. Wan, G. Taraschi, and Q. Zheng, Phys. Rev. Lett. **80**, 4277 (1998).